Hindawi
Mathematical Problems in Engineering
Volume 2019, Article ID 2723082, 11 pages
https://doi.org/10.1155/2019/2723082

Research Article

Shape Optimization and Stability Analysis for Kiewitt Spherical Reticulated Shell of Triangular Pyramid System

Le-Wen Zhang,[1] Jing Wu ,[1] and Da-Liang Zhang[2]

[1]*Institute of Marine Science and Technology, Shandong University, Qingdao, Shandong 266237, China*
[2]*Shandong Agriculture and Engineering University, Jinan, Shandong 250100, China*

Correspondence should be addressed to Jing Wu; jing.wu@sdu.edu.cn

Received 19 April 2019; Revised 13 June 2019; Accepted 23 June 2019; Published 18 July 2019

Academic Editor: Petr Krysl

The Kiewitt spherical reticulated shell of triangular pyramid system is taken as the object of this study; a macroprogram of parametric modeling is developed by using the ANSYS Parametric Design Language. The minimum structural total weight is taken as the objective function, and a shape optimization program is proposed and compiled by adopting the sequence two-stage algorithm in FORTRAN environment. Then, the eigenvalue buckling analysis for Kiewitt spherical reticulated shell of triangular pyramid system is carried out with the span of 90 m and rise-span ratio of 1/7~1/3. On this basis, the whole nonlinear buckling process of the structure is researched by considering initial geometrical imperfection. The load-displacement curves are drawn, and the nonlinear behaviors of special nodes are analyzed. The structural nonlinear behaviors affected by rise-span ratio are discussed. Finally, the stability of reticulated shell before and after optimization is compared. The research results show that (1) users can easily get the required models only by inputting five parameters, i.e., the shell span (S), rise (F), latitudinal portions (Kn), radial loops (Nx), and thickness (T). (2) Under the conditions of different span and rise-span ratio, the optimal grid number and bar section for the Kiewitt spherical reticulated shell of triangular pyramid system existed after optimization; i.e., the structural total weight is the lightest. (3) The whole rigidity and stability of the Kiewitt spherical reticulated shell of triangular pyramid system are very nice, and the reticulated shell after optimization can still meet the stability requirement. (4) When conducting the reticulated shell design, the structural stability and carrying capacity can be improved by increasing the rise-span ratio or the rise. (5) From the perspective of stability, the rise-span ratio of the Kiewitt spherical reticulated shell of triangular pyramid system should not choose 1/7.

1. Introduction

The reticulated shell is a major structural style of spatial structures, and it has advantages of reasonable force, rich structure type, convenient installation, etc., which has broad applications [1].

The spherical reticulated shell is a spatial structure of bar system, and its bar system is generated by connecting the nodes according to certain rules. It has the general characteristics of reticulated shell. More recently it has been widely used in large-span spatial structures, such as large-sized sports/arts venues, waiting rooms, and other landmark buildings. According to different grid types, there are six typical spherical reticulated shells, i.e., Ribbed spherical reticulated shell, Schwedler spherical reticulated shell, Lamella spherical reticulated shell, Three-way grid spherical reticulated shell, Kiewitt spherical reticulated shell, and Geodesic spherical reticulated shell. Among them, the Kiewitt spherical reticulated shell has the advantages of attractive appearance, reasonable force, low material consumption, large stiffness and span, etc., which has broad application prospects in modern buildings [2].

The Kiewitt spherical reticulated shell of triangular pyramid system combines the virtues of single-layer and double-layer spherical reticulated shells. It has higher integral bearing capacity and deformation resistant capability than those of single-layer spherical reticulated shell, and its total structural weight is less than that of double-layer spherical reticulated shell. Therefore, the Kiewitt spherical reticulated shell of triangular pyramid system is a new-type spatial structure, which can be widely applied in large-span architectures. However, the number of nodes and bar elements of reticulated shell is too many and the type of bar connection is

complicated. Moreover, the variation of span, rise, grid size, type, and other parameters can cause structural internal force reallocation. Thus, the workload of remodeling is very large when conducting shape optimization design and stability analysis. Conventional modeling of reticulated shell often focuses on hand-modeling in domestic and foreign studies. The studies of parametric modeling method based on the ANSYS Parametric Design Language (APDL) are not many, and relevant research rarely involves the specific work of shape optimization and stability analysis for the Kiewitt spherical reticulated shell of triangular pyramid system.

In the aspect of shape optimization, many optimized methods have been proposed, and the relevant studies are as follows. Zhang and Dong [3] presented a structural optimization algorithm and developed a computer program, and the effectiveness of the proposed method was verified. Wang and Tang [4] proposed an optimum method based on the optimality criteria, which could be used in optimization design of single-layer reticulated shells. Rahami *et al.* [5] introduced a combination of energy and force method and adopted the genetic algorithm for minimizing the weight of truss structures. Wu *et al.* [6] investigated a new design concept of MAS and proposed a shape optimization method with finite element analysis, which could be used in two-dimensional stent models. Luo et al. [7] also studied a meshless Galerkin level set method for shape and topology optimization of continuum structures. Yildiz [8] investigated a comparison of evolutionary-based optimization techniques and proposed a hybrid optimization technique based on differential evolution algorithm for structural design optimization problems. Wang et al. [9] proposed a new Multi-Material Level Set topology description model for topology and shape optimization of structures involving multiple materials. Lian et al. [10] developed a T-spline isogeometric boundary element method to conduct shape sensitivity analysis and gradient-based shape optimization in the three-dimensional linear elastomer. Lian et al. [11] showed that a combined shape and topology optimization method could produce optimal 2D designs with minimal stress subject to a volume constraint. Burman et al. [12] presented a cut finite element method for shape optimization in the case of linear elasticity. In addition, the publications [13–20] also involve the structural optimization design.

In the early days, people adopted the imitative shell method based on continuous medium theory to analyze the stability of reticulated shell [21]. Although this method plays an important role in analyzing the stability of reticulated shell of particular form, it also has some limitations. With the speedy development of computer technology, the nonlinear finite element analysis has become a universal approach for structural stability analysis [22]. During the stability analysis of reticulated shell, the strength and stability are considered independently, which is usually adopted by the traditional linear analysis method. However, the above two factors are considered simultaneously in the nonlinear full-range analysis, so the load-displacement curve can be drawn accurately, and the impacts of various factors on structural stability can be analyzed reasonably.

In terms of structural stability analysis, the research on eigenvalue buckling analysis and nonlinear buckling analysis has got some achievements. Ferreira and Barbosa [23] presented a finite-element model for geometric nonlinear analysis of composite shell structures. Han *et al.* [24] investigated the validity of the finite element method on the buckling and post-buckling behavior of laminated composite cylindrical shells that have been subjected to an external hydrostatic pressure. Basaglia *et al.* [25] adopted the generalized beam theory (GBT) to analyze the global buckling behavior of plane and space thin-walled frames. Papadopoulos *et al.* [26] presented a computationally efficient method for the buckling analysis of shells with random imperfections, based on a linearized buckling approximation of the limit load of the shell. Ghannadpour and Ovesy [27] presented theoretical developments of an exact finite strip for the buckling analysis of symmetrically laminated composite plates and plate structures. Camotim et al. [28] presented a state-of-the-art report on the use of GBT to assess the buckling behavior of plane and space thin-walled steel frames. Alibrandi *et al.* [29] proposed an efficient procedure for the reliability analysis of frame structures with respect to the buckling limit state. Fekrar *et al.* [30] conducted the buckling analysis of functionally graded hybrid composite plates by using a new four-variable refined plate theory. Wang and Peng [31] proposed a Hermite reproducing kernel Galerkin meshfree approach for buckling analysis of thin plates. Ovesy *et al.* [32] presented an exact finite strip for the buckling analysis of laminated composite plates and plate structures by using First-order Shear Deformation Theory. Basaglia and Camotim [33] dealt with the application of beam finite element models based on GBT to analyze the buckling behavior of four thin-walled steel structural systems. Zhou *et al.* [34] revisited the buckling analysis of a benchmark cylindrical panel undergoing snap-through when subjected to transverse loads. Ghannadpour et al. [35] presented an exact finite strip for the buckling and post-buckling analysis of moderately thick plates by using the First order Shear Deformation Theory. Kandasamy et al. [36] studied the free vibration and thermal buckling behavior of moderately thick functionally graded material structures including plates, cylindrical panels, and shells under thermal environments. Çelebi *et al.* [37] conducted the evaluation of the buckling and failure characteristics of shells include linear buckling analysis and nonlinear failure analysis using Riks method.

In the present study, a parametric modeling macroprogram for the Kiewitt spherical reticulated shell of triangular pyramid system is developed by using the APDL. On this basis, a shape optimization program is compiled by adopting the sequence two-stage algorithm in FORTRAN environment. Shape optimization is achieved based on the objective function of minimizing total structural weight and the restriction condition of global constraints, locality constraints. Then, stability analysis for the Kiewitt spherical reticulated shell of triangular pyramid system is carried out with the span of 90 m and rise-span ratio of 1/7~1/3. The stability analysis includes linear buckling analysis and nonlinear buckling analysis. Finally, the stability of reticulated shell before and after optimization is compared by examples.

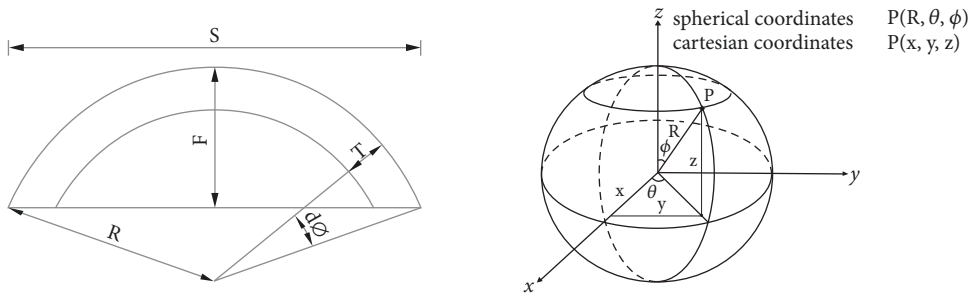

Figure 1: Schematic diagram of geometric parameters of spherical reticulated shell.

The conclusions of having reference significance for practical engineering are obtained.

2. Parametric Modeling for Kiewitt Spherical Reticulated Shell of Triangular Pyramid System

2.1. Geometric Descriptions. The span (S), rise (F), latitudinal portions (Kn), radial loops (Nx), and thickness (T) are the main geometric parameters of describing spherical reticulated shell [14, 15]. The schematic diagram of geometric parameters of spherical reticulated shell is shown in Figure 1.

The sphere curvature radius R is calculated as follows:

$$R = \frac{S^2/4 + F^2}{2F} \tag{1}$$

The global angle $Dpha$ of two radial neighboring circle nodes is calculated as follows:

$$Dpha = \begin{cases} \dfrac{1}{Nx} \arctan\left(\dfrac{S/2}{\sqrt{R^2 - (S/2)^2}}\right) & \dfrac{F}{S} \neq \dfrac{1}{2} \\ \dfrac{90}{Nx} & \dfrac{F}{S} = \dfrac{1}{2} \end{cases} \tag{2}$$

2.2. Parametric Modeling. S, F, Kn, Nx, and T are determined in the spherical coordinates; then the R and $Dpha$ are calculated. The nodes are generated in each circle from inside to outside in order by using cyclic command statements. Let vertex of upper layer be number 1. Then the numbers and coordinates of nodes are calculated. The bar element is generated by connecting related nodes according to the following conventions: applying loads on nodes whose number is less than starting node number of the outermost circle and imposing displacement constraints on other nodes. A macroprogram of parametric modeling is compiled by using APDL. The specific parametric modeling process can refer to Wu *et al.* [14, 15].

2.3. The Input Window of Geometrical Parameters and Modeling Examples. A program for input window of geometrical parameters is compiled by using APDL, and the input window is shown in Figure 2. Users can easily get the required models only by inputting the parameters such as S, F, Kn, Nx, and T.

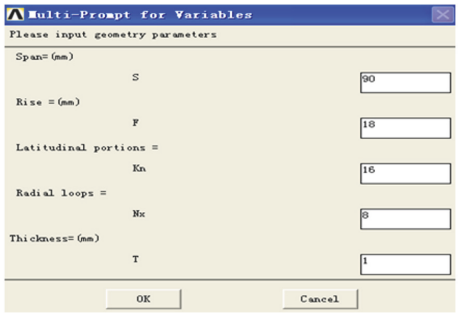

Figure 2: Input window of geometrical parameters.

Some parametric modeling examples of Kiewitt spherical reticulated shell are given in Figures 3-4.

3. Shape Optimization for the Kiewitt Spherical Reticulated Shell of Triangular Pyramid System

3.1. Mathematical Models of Shape Two-Stage Optimization. The mathematical models of shape optimization mainly include design variables, objective function, and constraint conditions. The detailed information can be referred in Wu et al.'s previous studies [14, 15].

(1) The First-Stage (Cross-Section) Optimization. Mathematical models of cross-section optimization are as follows:

$$\begin{aligned} & P_1 \quad Seeking\ A \\ & \min \quad W = \sum_{i=1}^{m} \rho_i l_i (S)\, Ai + \sum_{j=1}^{n} \rho_j V_j \\ & s.t. \quad \sigma_{wi} \leq [\sigma] \\ & \qquad \lambda_i \leq [\lambda] \\ & \qquad x_i \in S_i \end{aligned} \tag{3}$$

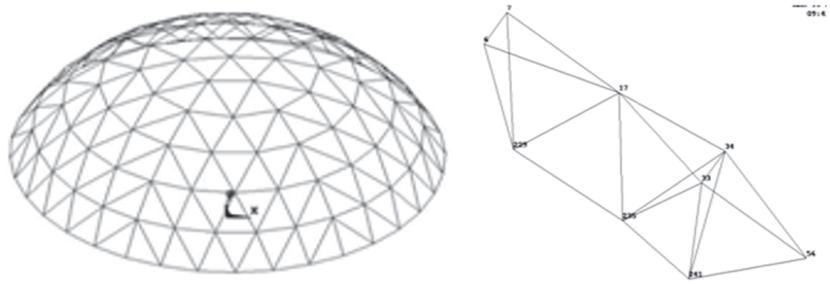

(a) Single-layer (b) Triangular pyramid system

Figure 3: Kiewitt spherical reticulated shell.

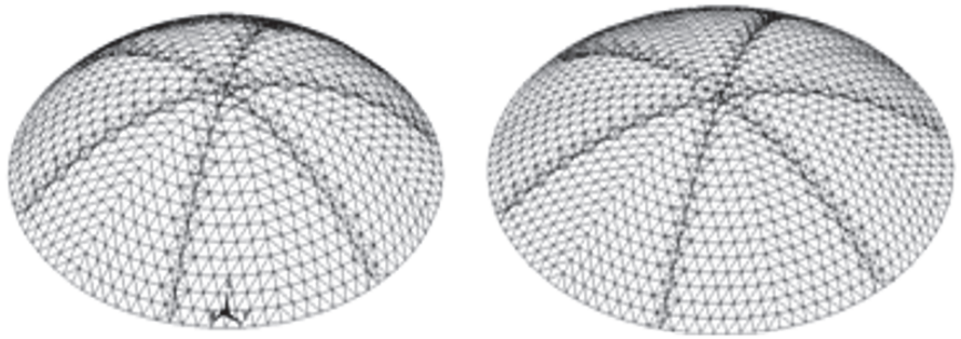

(a) S=60; F=15; Kn=6; Nx=16; T=1.0 (b) S=90; F=18; Kn=6; Nx=18; T=1.5

Figure 4: Kiewitt spherical reticulated shell of triangular pyramid system.

(2) The Second-Stage (Shape) Optimization. Mathematical models of shape optimization are as follows:

$$\begin{aligned} P_2 \quad & Seeking\ Kn,\ Nx,\ T \\ \min \quad & W = \sum_{i=1}^{m} \rho_i l_i\,(Kn,\ Nx,\ T)\, A_i + \sum_{j=1}^{n} \rho_j V_j \qquad (4) \\ s.t. \quad & \delta_{\max} \le [\delta] \end{aligned}$$

Given the range of Kn, Nx, and T, the optimal solution is sought with the goal of minimizing the total weight of spherical reticulated shell.

3.2. Process of Shape Optimization. The design concept of two-stage optimization can refer to Wu et al. [18].

The specific process of cross-section optimization is described as follows:

(1) Modeling is conducted in the ANSYS software, and S, F, Kn, Nx, and T are input. The loads and boundary constraints are applied on the model. The bar elements are divided into many groups and the material characteristics are input, respectively. Mechanical analysis is carried out and pretreatment files are generated.

(2) Input the number of nodes and bar elements, the grouping number, the types of ball joint, the discrete sets of node and bar element types, and other basic parameters in program.

(3) The first element of the discrete sets is selected as initial design variables, and the corresponding cross-sectional area of bar element in the pretreatment files is replaced. One-dimensional searching is conducted.

(4) Internal force analysis of the structure is carried out by calling interface program, in order to check constraints of stress, displacement, and slenderness ratio. If they meet the constraints, then turn to step (7). If not, turn to step (5).

(5) The second level cross-section optimization is carried out.

(6) Internal force analysis of the structure is carried out by calling interface program, in order to check constraints of stress, displacement, and slenderness ratio. If they meet the constraints, then turn to step (7). If not, calculate relative difference quotient and form new design point; then turn to step (5).

(7) Conduct Zeroth correction, and output optimization results (cross-sectional area of bar elements).

(8) Ball joints are selected and optimized according to the optimal cross-sectional area of bar elements.

(9) Output the whole optimization results, and the program runs to completion.

The cross-section optimization flowchart of Kiewitt spherical reticulated shell of triangular pyramid system is shown in Figure 5.

3.3. Results of Shape Optimization. The bar elements of spherical reticulated shell adopt hot-rolling seamless pipe,

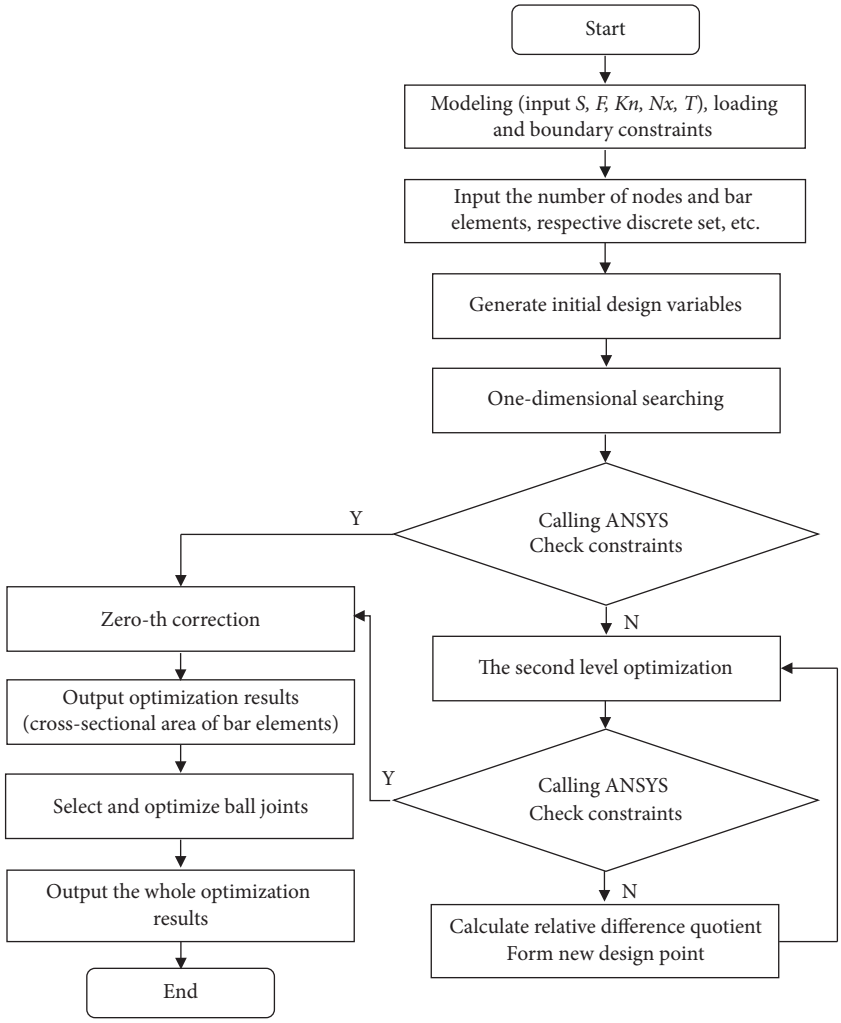

Figure 5: Cross-section optimization flowchart of Kiewitt spherical reticulated shell of triangular pyramid system.

steel density ρ= 7800 kg/m^3, elastic modulus E = 2.06 × 10^5 Mpa, Poisson ratio ε=0.3, and yield strength of steel [σ] =2.15 × 10^{8}N/m^2. The steel type is Q235; i.e., outer diameter D=0.152m, wall thickness t=5mm, sectional area S=2.309 × 10-3m^2, second moment of area I=6.2443 × 10-6m^4, and sectional resistance moment W= 8.216 × 10^{-5}m^3. The uniform load (q = 2.35 KN/m^2) has vertically downward effect on the nodes of spherical reticulated shell. In addition, constraint conditions of the outermost nodes of spherical reticulated shell are simply supported. The optimized results of Kiewitt spherical reticulated shell of triangular pyramid system with the span of 90 m are shown in Table 1.

4. Stability Analysis for the Kiewitt Spherical Reticulated Shell of Triangular Pyramid System

The eigenvalue buckling analysis and geometric nonlinear analysis for Kiewitt spherical reticulated shell of triangular pyramid system are carried out in this section. The structural load-displacement curve is got, and the whole changing process of structural displacement is fully understood by response analysis. The structural stability capacity is determined, and the relationship between displacement and stability is discussed.

4.1. Eigenvalue (Linear) Buckling Analysis. Buckling analysis is mainly used for studying structural stability under specific loads and determining the critical load of structural instability. The buckling analysis includes linear buckling analysis and nonlinear buckling analysis. The linear elastic buckling analysis is also known as the eigenvalue buckling analysis. The nonlinear buckling analysis includes geometrical nonlinear buckling analysis, elastic-plastic buckling analysis, and nonlinear post-buckling analysis.

The purpose of eigenvalue buckling analysis is to predict theoretical buckling strength of an ideal elastomer, which is similar to buckling analysis of elasticity theory. However, initial imperfection and nonlinear behavior existed in practical reticulated shells. The linear analysis method overestimates the structural load-carrying capacity, so the solution of eigenvalue buckling analysis is very conservative and not safe. But the primary advantage of this approach is

Table 1: Optimal results of Kiewitt spherical reticulated shell of triangular pyramid system.

Span/m	Rise-span ratio/1	The range of grids		Optimal grid number		Optimal thickness/m	Optimal weight/t	Optimal solution
		Kn	*Nx*	*Kn*	*Nx*			*S-F/S-Kn-Nx*
90	1/7	6/8/10/12	12~20	6	14	1.5	185.43	90-1/5-8-15
	1/6	6/8/10/12	12~20	6	14	1.0	180.51	
	1/5	6/8/10/12	12~20	8	15	1.0	147.14	
	1/4	6/8/10/12	12~20	6	15	1.5	159.60	
	1/3	6/8/10/12	12~20	6	16	1.0	186..84	

Table 2: Eigenvalue buckling loading coefficients of first six order modes.

Rise-span ratio/1	The first six order modes					
	1	2	3	4	5	6
1/7	5.018	5.019	5.019	5.022	5.022	5.025
1/6	6.542	6.547	6.547	6.554	6.554	6.560
1/5	8.830	8.833	8.833	8.839	8.839	8.843
1/4	12.273	12.277	12.277	12.282	12.282	12.282
1/3	15.663	15.664	15.644	15.665	15.665	15.665

that the analysis process adopts linear computation, and the calculation speed is fast, which can provide a basis for further analysis and determination of the critical load. Therefore, the eigenvalue buckling analysis conducted in advance will contribute to the following nonlinear buckling analysis, and it is the foundation for further geometric nonlinear analysis.

The eigenvalue buckling load is the upper critical point of the linear buckling load, and it can be used as a given load of nonlinear buckling analysis. Feature vector buckling shapes can be used as a basis for applying initial imperfection or disturbance loads.

The eigenvalue can be obtained by the load factor or the scale factor in the flowing equation:

$$\left([K] + \lambda \left[K_s\right]\right)\{\varphi\} = 0 \tag{5}$$

where [K] is the stiffness matrix; [Ks] is the stress stiffness matrix; φ is the vector of displacement; λ is the eigenvalue.

The λ represents the scale factor of a given load. If the given load is a unit load, then the resulting eigenvalue is the buckling load of the reticulated shell.

The eigenvalue (linear) buckling analysis for Kiewitt spherical reticulated shell of triangular pyramid system is carried out with the span of 90 m and rise-span ratio of 1/7~1/3. The calculation parameters can refer to Section 3.3. Linear buckling loading coefficients of the first six order modes with the rise-span ratio of 1/7~1/3 are listed in Table 2. The first three order modes and buckling loading coefficients with the rise-span ratio of 1/5 are shown in Figures 6–8.

It can be obtained from Table 2 and Figures 6–8:

(1) During the eigenvalue buckling analysis, the eigenvalue buckling loading coefficient that corresponded by each order mode increases with the rise-span ratio. It can be generally inferred that the stability of Kiewitt spherical reticulated shell of triangular pyramid system increases with the span-rise ratio. Moreover, the influence of rise-span ratio on eigenvalue buckling loading coefficient is very large. Take the first order mode for an example: the eigenvalue buckling load coefficient is 5.018 when the rise-span ratio is 1/7, while the eigenvalue buckling load coefficient increases to 15.663 when the rise-span ratio is 1/3, which has more than tripled.

(2) As for the first three order modes that corresponded by each rise-span ratio, the eigenvalue buckling load coefficients of the second order mode and the third order mode are the same, but they are different from that of the first order mode. The integral structural buckling modes of the second order and the third order are positive symmetric, while the first order mode is antisymmetric. The main reason is that the shape of reticulated shell and load distribution are symmetrical.

4.2. Geometrical Nonlinear Whole-Process Analysis

(1) Structural Nonlinear Whole-Process Analysis with Initial Geometrical Imperfection. The geometrical nonlinear buckling analysis is to use the finite element method to analyze the structural stability. The geometrical nonlinear whole-process analysis can be conducted through load-displacement curves, and then the structural carrying capacity can be determined.

The nonlinear buckling analysis for Kiewitt spherical reticulated shell of triangular pyramid system is carried out by consideration of initial geometrical imperfection, and the geometrical nonlinear whole process is analyzed.

After the stability whole-process analysis, the load-displacement curve of each node can be obtained. In general, the load-displacement curve of the maximum displacement node at the end of iteration is taken as a representative. The whole-process analysis curve is very complex. From the perspective of practicability, the equilibration stage and the subsequent buckling path are just taken and researched. During the nonlinear whole-process analysis, the relevant geometrical parameters are the same as the parameters of

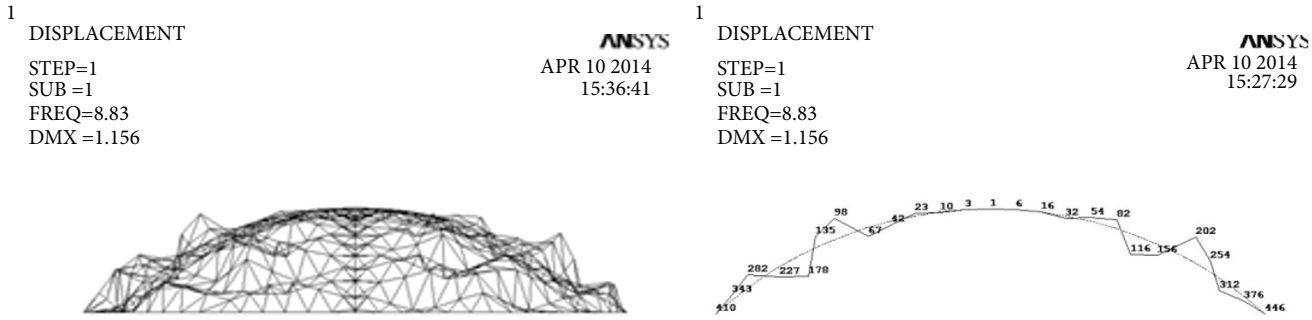

(a) The first order mode (b) The buckling loading coefficient, 8.830

Figure 6: The first order mode and buckling loading coefficient with the rise-span ratio of 1/5.

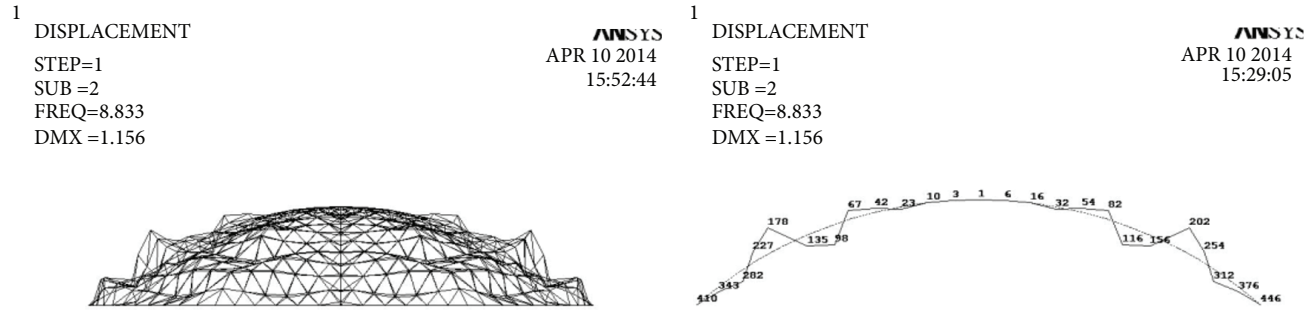

(a) The second order mode (b) The buckling loading coefficient, 8.833

Figure 7: The first order mode and buckling loading coefficient with the rise-span ratio of 1/5.

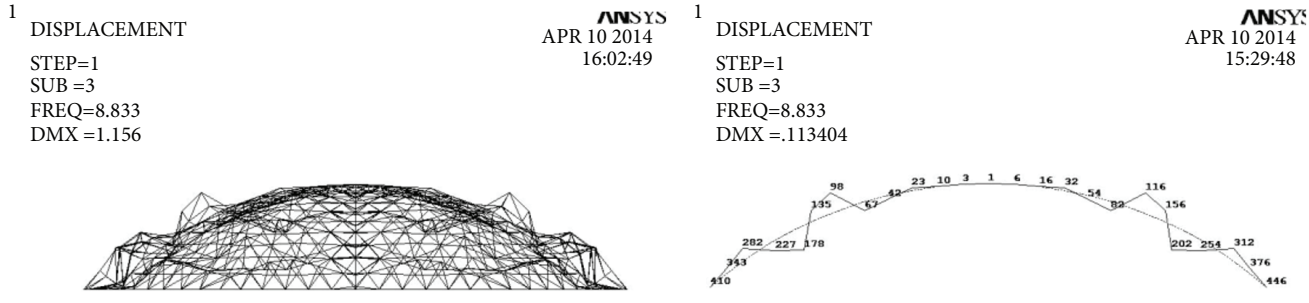

(a) The third order mode (b) The buckling loading coefficient, 8.833

Figure 8: The first order mode and buckling loading coefficient with the rise-span ratio of 1/5.

eigenvalue buckling analysis. Take 1/300 of span (90m) as the initial geometrical imperfection, and it is applied on the Kiewitt spherical reticulated shell of triangular pyramid system for nonlinear buckling analysis. The node 77 is located on the main rib of the 4-th loop from the vertex to outside, and its displacement is the largest. The nodes 76 and 78 are adjacent to the node 77, and they are located on the same loop. The load-displacement curves of the three nodes are shown in Figure 9. The curve is complex and varied, but with good regularity.

It can be reached from Figure 9:

(1) The relationship between the load and displacement is basically linear at the initial stage of loading (i.e., equilibrium path stage). After the upper critical point, the structure enters the post-buckling stage, and the relationship between the load and displacement is obviously nonlinear.

(2) When the structure reaches the upper critical point, the Z direction displacements of the three nodes (76, 77, and 78) are 0.07m, 0.19m, and 0.07m. After the post-buckling stage, the Z direction displacements of the three nodes (76, 77, and 78) are 0.69m, 1.00m, and 0.69m based on the computation convergence. With the node 77, for example, when the post-buckling path reaches the first lower critical point, the displacement is 0.45m. The value has exceeded structural maximum allowable value (span/400=0.225m) according to the architectural structure load code. In the later stages, the displacement that corresponded by each limit point far exceeds the maximum allowable value (0.225). Therefore,

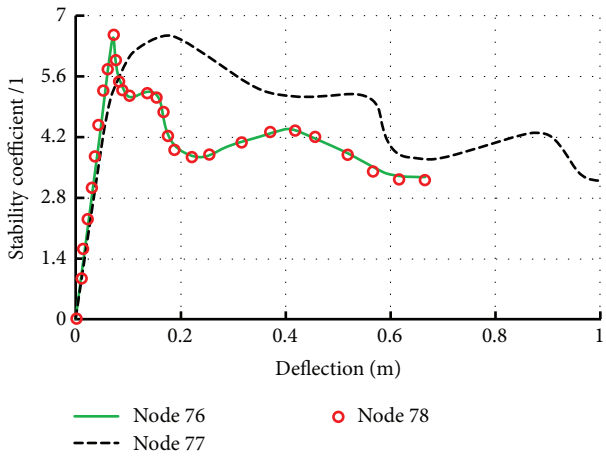

Figure 9: Load-displacement curves of the nodes (76, 77, and 78) with the rise-span ratio of 1/5.

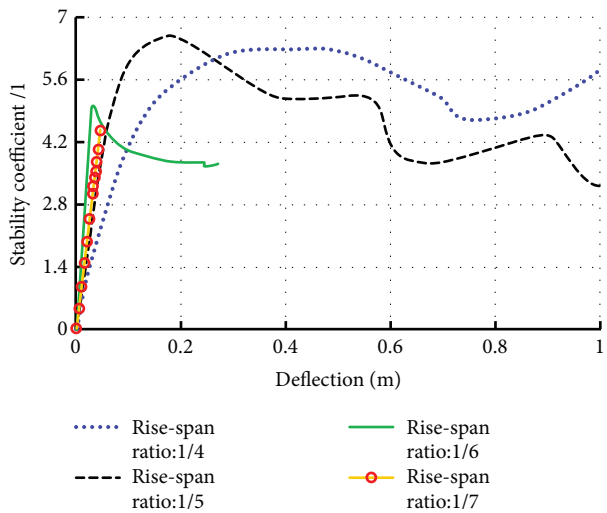

Figure 10: Load-displacement curves of the node 77 with the rise-span ratio of 1/4~1/7.

the following paths after the first lower critical point have no practical engineering significance for studying reticulated shell.

(3)As far as these three nodes are concerned, the node 77 is the first to buckling. When the structure reaches the ultimate bearing capacity and begins to collapse, the Z direction displacement of node 77 is the largest, and the displacements of nodes 76 and 78 are the same. That is mainly because the two nodes (76 and 78) are symmetrically located on both sides of the node 77.

(4) When the structure reaches the upper critical point, the maximum Z direction displacement is 0.19m, which is 1/450 of the structural span (S=90m). The structural maximum displacement must not exceed 1/400 of the span based on the architectural structure load code, so the displacement meets the relevant requirement of reticulated shell. The stability coefficient of reticulated shell is 6.54. The stability coefficient must not be less than 4.2 according to the technical specification for reticulated shell and design code for the steel structures, so the stability meets the requirement. In conclusion, it can be drawn that the whole rigidity and stability of Kiewitt spherical reticulated shell of triangular pyramid system are relatively good.

(2) Structural Nonlinear Buckling Analysis in Different Rise-Span Ratio. In order to investigate the structural nonlinear buckling affected by the rise-span ratio, the rise-span ratio of reticulated shell is set as 1/4, 1/5, 1/6, and 1/7, respectively, and the structural nonlinear buckling process is analyzed. The load-displacement curves of the node 77 (the maximum displacement node) with the rise-span ratio of 1/4~1/7 are shown in Figure 10.

It can be reached from Figure 10:

(1) For the Kiewitt spherical reticulated shell of triangular pyramid system, the load-displacement curves vary greatly in different rise-span ratio. But their common feature is that the equilibrium path before reaching the upper critical point is nearly linear, and the displacement is small. For the post-buckling stage, the curves come in all shapes and sizes, but they converge eventually. During the post-buckling stage, the displacement increases rapidly.

(2) The stability coefficient of reticulated shell changes with the rise-span ratio, and the stability coefficient is the largest when the rise-span ratio is 1/5.

(3) Within a certain range, the larger the rise-span ratio, the greater the critical bearing capacity. Going even further, the bearing capacity and deformation capacity of the post-buckling stage are also greater. Therefore, when conducting reticulated shell design, the structural stability and bearing capacity can be improved by increasing the rise-span ratio or rise appropriately.

(4) When the rise-span ratio is 1/7, the corresponding stability coefficient is 4.45. Although the value can meet the relevant requirements of specification, it is close to the allowable value 4.2. Moreover, the displacement is only 0.0345m when reticulated shell converges eventually. At the moment, the structural deformation capacity is much of poor. Therefore, from the perspective of stability, the structural rise-span ratio should not choose 1/7 in practical engineering.

In addition, the stability of the optimized Kiewitt spherical reticulated shell of triangular pyramid system is analyzed. The optimal geometrical parameters after optimization are as follows: The rise-span ratio is 1/5; the latitudinal portions are 8 (Kn=8); and the radial loops are 15 (Nx=15). The optimal values of bar section are shown in Table 3.

The optimized sectional dimensions are given to the bar elements, and then the structural nonlinear buckling analysis is carried out. The load-displacement curves are drawn, as shown in Figure 11.

It can be known from Figure 11: The structural stability coefficient is 6.33 before optimization, while it is 4.28 after optimization. The stability coefficient became smaller. That is to say that the safety stock of reticulated shell is reduced on the premise of satisfying the design requirements of structural global stability. The main reason is that the total weight of optimized reticulated shell is reduced. However, the

Table 3: Optimal values of bar section.

The number of bar group	The optimal bar section	The number of bar group	The optimal bar section	The number of bar group	The optimal bar section
1	ϕ 108 × 4	12	ϕ 133 × 4	23	ϕ 114 × 4
2	ϕ 127 × 4	13	ϕ 89 × 3.5	24	ϕ 121 × 4
3	ϕ 127 × 4	14	ϕ 127 × 4	25	ϕ 114 × 4
4	ϕ 102 × 4	15	ϕ 127 × 4	26	ϕ 121 × 4
5	ϕ 133 × 4.5	16	ϕ 127 × 4	27	ϕ 114 × 4
6	ϕ 133 × 4.5	17	ϕ 127 × 4	28	ϕ 108 × 4
7	ϕ 121 × 4	18	ϕ 102 × 3.5	29	ϕ 114 × 4
8	ϕ 102 × 3.5	19	ϕ 121 × 4	30	ϕ 194 × 5
9	ϕ 121 × 4	20	ϕ 102 × 3.5	31	ϕ 114 × 4
10	ϕ 102 × 3.5	21	ϕ 121 × 4		
11	ϕ 95 × 3.5	22	ϕ 121 × 4		

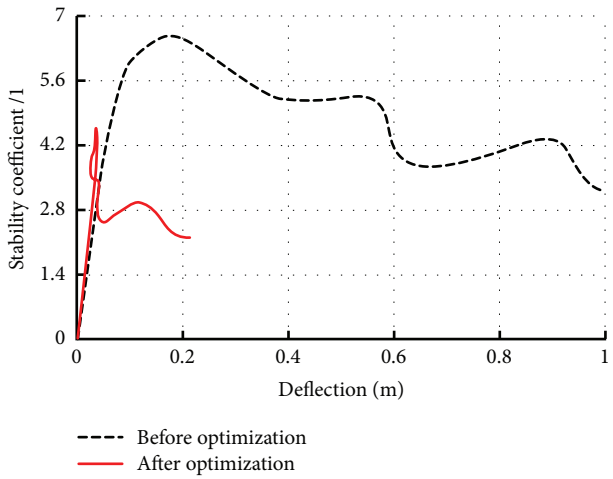

Figure 11: Load-displacement curves of the node 77 before and after optimization (rise-span ratio, 1/5).

optimized stability coefficient is still higher than the limiting value in the technical specification of reticulated shell. It shows that the optimized reticulated shell still satisfies the safety requirement specified by the code.

5. Conclusions

An efficient parametric modeling method is proposed for the Kiewitt spherical reticulated shell of triangular pyramid system. A shape optimization program is compiled by using sequence two-stage algorithm in FORTRAN environment. The eigenvalue buckling analysis for Kiewitt spherical reticulated shell of triangular pyramid system is carried out with the span of 90 m and rise-span ratio of 1/7~1/3. On this basis, the structural nonlinear buckling whole-process is researched by considering initial geometrical imperfection. Some useful conclusions are drawn as follows:

(i) Users can easily get the required models only by inputting five parameters, i.e., the shell span (S), rise (F), latitudinal portions (Kn), radial loops (Nx), and thickness (T).

(ii) Under the conditions of different span and rise-span ratio, the optimal grid number and bar section of Kiewitt spherical reticulated shell of triangular pyramid system existed after optimization. Moreover, at this moment, the total weight is the lightest.

(iii) The whole rigidity and stability of Kiewitt spherical reticulated shell of triangular pyramid system are very good, and the optimized reticulated shell can still meet stability requirements.

(iv) The stability and carrying capacity can be improved by increasing rise-span ratio or rise when conducting design of reticulated shell.

(v) From the perspective of stability, the rise-span ratio of Kiewitt spherical reticulated shell of triangular pyramid system should not choose 1/7.

Data Availability

The data used to support the findings of this study are available from the corresponding author upon request.

Conflicts of Interest

The authors declare that they have no conflicts of interest.

Acknowledgments

The authors would like to acknowledge the financial support from the China Postdoctoral Science Foundation (Grant No.: 2019M652384) and the Natural Science Foundation of Shandong Province (Grant No.: ZR2017MEE032).

References

[1] S. L. Dong and J. Yao, "Future and prospects of reticulated shells," *Spatial Structure*, vol. 9, no. 1, pp. 31–34, 2003.

[2] X. Y. Lu, X. W. Zhao, L. L. Huang, Q. Wang, and C. Wang, "Shape optimizing design of kiewiti spherical reticulated shell," *Advanced Materials Research*, vol. 424-425, pp. 324–329, 2012.

[3] N. W. Zhang and S. L. Dong, "Optimum design of single-layer lattice shells considering the effect of geometrical nonlinearity," *Spatial Structure*, vol. 9, no. 1, pp. 31–34, 2003.

[4] C. W. Wang and G. Tang, "Sectional optimum design of single-layer lattice shells considering structural stability," *Spatial structure*, vol. 12, no. 3, pp. 31–34, 2006.

[5] H. Rahami, A. Kaveh, and Y. Gholipour, "Sizing, geometry and topology optimization of trusses via force method and genetic algorithm," *Engineering Structures*, vol. 30, no. 9, pp. 2360–2369, 2008.

[6] W. Wu, L. Petrini, D. Gastaldi et al., "Finite element shape optimization for biodegradable magnesium alloy stents," *Annals of Biomedical Engineering*, vol. 38, no. 9, pp. 2829–2840, 2010.

[7] Z. Luo, N. Zhang, W. Gao, and H. Ma, "Structural shape and topology optimization using a meshless Galerkin level set method," *International Journal for Numerical Methods in Engineering*, vol. 90, no. 3, pp. 369–389, 2012.

[8] A. R. Yildiz, "Comparison of evolutionary-based optimization algorithms for structural design optimization," *Engineering Applications of Artificial Intelligence*, vol. 26, no. 1, pp. 327–333, 2013.

[9] Y. Q. Wang, Z. Luo, Z. Kang, and N. Zhang, "A multi-material level set-based topology and shape optimization method," *Computer Methods Applied Mechanics and Engineering*, vol. 283, pp. 1570–1586, 2015.

[10] H. Lian, P. Kerfriden, and S. P. A. Bordas, "Shape optimization directly from CAD: an isogeometric boundary element approach using T-splines," *Computer Methods Applied Mechanics and Engineering*, vol. 317, pp. 1–41, 2017.

[11] H. J. Lian, A. N. Christiansen, D. A. Tortorelli, O. Sigmund, and N. Aage, "Combined shape and topology optimization for minimization of maximal von Mises stress," *Structural and Multidisciplinary Optimization*, vol. 55, no. 5, pp. 1541–1557, 2017.

[12] E. Burman, D. Elfverson, P. Hansbo, M. G. Larson, and K. Larsson, "Shape optimization using the cut finite element method," *Computer Methods Applied Mechanics and Engineering*, vol. 328, pp. 242–261, 2018.

[13] A. P. Thrall, M. Zhu, J. K. Guest, I. Paya-Zaforteza, and S. Adriaenssens, "Structural optimization of deploying structures composed of linkages," *Journal of Computing in Civil Engineering*, vol. 28, no. 3, Article ID 04014010, 2012.

[14] J. Wu, X. Y. Lu, S. C. Li et al., "Shape optimization for partial double-layer spherical reticulated shells of pyramidal system," *Structural Engineering and Mechanics*, vol. 55, no. 3, pp. 555–581, 2015.

[15] J. Wu, X. Y. Lu, S. C. Li et al., "Parametric modeling and shape optimization of four typical Schwedler spherical reticulated shells," *Structural Engineering and Mechanics*, vol. 56, no. 5, pp. 813–833, 2015.

[16] D. J. Munk, G. A. Vio, and G. P. Steven, "Topology and shape optimization methods using evolutionary algorithms: a review," *Structural and Multidisciplinary Optimization*, vol. 52, no. 3, pp. 613–631, 2015.

[17] J.-H. Zhu, P. Beckers, M. Dahan, J. Yan, and C. Jiang, "Shape and topology optimization for complicated engineering structures," *Mathematical Problems in Engineering*, vol. 2015, Article ID 723897, 2 pages, 2015.

[18] J. Wu, X. Y. Lu, S. C. Li et al., "Parametric modeling and shape optimization design of five extended cylindrical reticulated shells," *Steel and Composite Structures*, vol. 21, no. 1, pp. 217–247, 2016.

[19] W. S. Zhang, J. Zhang, and X. Guo, "Lagrangian description based topology optimization-a revival of shape optimization," *Journal of Applied Mechanics*, vol. 83, no. 4, Article ID 041010, 2016.

[20] D. Jasińska and D. Kropiowska, "The optimal design of an arch girder of variable curvature and stiffness by means of control theory," *Mathematical Problems in Engineering*, vol. 2018, Article ID 8239464, 13 pages, 2018.

[21] E. Maiorana and C. Pellegrino, "Linear buckling analysis of welded girder webs with variable thickness," *Steel and Composite Structures*, vol. 11, no. 6, pp. 505–524, 2011.

[22] Y. Zhao, M. Chen, F. Yang, L. Zhang, and D. Fang, "Optimal design of hierarchical grid-stiffened cylindrical shell structures based on linear buckling and nonlinear collapse analyses," *Thin-Walled Structures*, vol. 119, pp. 315–323, 2017.

[23] A. J. M. Ferreira and J. T. Barbosa, "Buckling behaviour of composite shells," *Composite Structures*, vol. 50, no. 1, pp. 93–98, 2000.

[24] J. Y. Han, H. Y. Jung, J. R. Cho, J. H. Choi, and W. B. Bae, "Buckling analysis and test of composite shells under hydrostatic pressure," *Journal of Materials Processing Technology*, vol. 201, no. 1-3, pp. 742–745, 2008.

[25] C. Basaglia, D. Camotim, and N. Silvestre, "Global buckling analysis of plane and space thin-walled frames in the context of GBT," *Thin-Walled Structures*, vol. 46, no. 1, pp. 79–101, 2008.

[26] V. Papadopoulos, D. C. Charmpis, and M. Papadrakakis, "A computationally efficient method for the buckling analysis of shells with stochastic imperfections," *Computational Mechanics*, vol. 43, no. 5, pp. 687–700, 2009.

[27] S. A. M. Ghannadpour and H. R. Ovesy, "The application of an exact finite strip to the buckling of symmetrically laminated composite rectangular plates and prismatic plate structures," *Composite Structures*, vol. 89, no. 1, pp. 151–158, 2009.

[28] D. Camotim, C. Basaglia, and N. Silvestre, "GBT buckling analysis of thin-walled steel frames: A state-of-the-art report," *Thin-Walled Structures*, vol. 48, no. 10-11, pp. 726–743, 2010.

[29] U. Alibrandi, N. Impollonia, and G. Ricciardi, "Probabilistic eigenvalue buckling analysis solved through the ratio of polynomial response surface," *Computer Methods Applied Mechanics and Engineering*, vol. 199, no. 9-12, pp. 450–464, 2010.

[30] A. Fekrar, N. El Meiche, A. Bessaim, A. Tounsi, and E. A. Adda Bedia, "Buckling analysis of functionally graded hybrid composite plates using a new four variable refined plate theory," *Steel and Composite Structures*, vol. 13, no. 1, pp. 91–107, 2012.

[31] D. Wang and H. Peng, "A Hermite reproducing kernel Galerkin meshfree approach for buckling analysis of thin plates," *Computational Mechanics*, vol. 51, no. 6, pp. 1013–1029, 2013.

[32] H. R. Ovesy, S. A. M. Ghannadpour, and E. Zia-Dehkordi, "Buckling analysis of moderately thick composite plates and plate structures using an exact finite strip," *Composite Structures*, vol. 95, pp. 697–704, 2013.

[33] C. Basaglia and D. Camotim, "Buckling analysis of thin-walled steel structural systems using generalized beam theory (GBT)," *International Journal of Structural Stability and Dynamics*, vol. 15, no. 1, Article ID 1540004, 2015.

[34] Y. Zhou, I. Stanciulescu, T. Eason, and M. Spottswood, "Nonlinear elastic buckling and postbuckling analysis of cylindrical

panels," *Finite Elements in Analysis and Design*, vol. 96, pp. 41–50, 2015.

[35] S. A. M. Ghannadpour, H. R. Ovesy, and E. Zia-Dehkordi, "Buckling and post-buckling behaviour of moderately thick plates using an exact finite strip," *Computers & Structures*, vol. 147, pp. 172–180, 2015.

[36] R. Kandasamy, R. Dimitri, and F. Tornabene, "Numerical study on the free vibration and thermal buckling behavior of moderately thick functionally graded structures in thermal environments," *Composite Structures*, vol. 157, pp. 207–221, 2016.

[37] M. Çelebi, Z. Gürdal, and H. S. Türkmen, "Buckling analysis of CFRP composite cylindrical shell with cutouts in bending," *Journal of Aeronautics and Space Technologies*, vol. 10, no. 2, pp. 7–15, 2017.